Heart and Vessels (2019) 34:2041–2051
https://doi.org/10.1007/s00380-019-01452-8

ORIGINAL ARTICLE

Regulation mechanism of aquaporin 9 gene on inflammatory response and cardiac function in rats with myocardial infarction through extracellular signal-regulated kinase1/2 pathway

Xingmei Huang[1] · Xiaobin Yu[2] · Hongxia Li[1] · Lianhua Han[1] · Xiangjun Yang[1]

Received: 1 December 2018 / Accepted: 14 June 2019 / Published online: 19 June 2019

Abstract

The aim of this study was to investigate the regulation mechanism of aquaporin 9 (AQP9) gene on inflammatory response and cardiac function in rats with myocardial infarction (MI) through extracellular signal-regulated kinase1/2 (ERK1/2) pathway. The constructed rats models of MI were randomly divided into 6 groups: control group (sham operation group, MI modeling sham operation), model group (MI modeling), NC group (MI modeling, tail vein injection of AQP9 negative control sequence vector), AQP9 shRNA group (MI modeling, tail vein injection of AQP9 shRNA plasmid vector), U0126 group (MI modeling, tail vein injection of ERK signaling pathway inhibitor), and AQP9 shRNA + U0126 group. The hemodynamics and cardiac function of rats in each group were detected on the seventh day of modeling. The levels of AQP9 and inflammatory factors [tumour necrosis factor-α (TNF-α), interleukin-6 (IL-6), interleukin-10 (IL-10)] in peripheral blood of rats were detected by ELISA method. qRT-PCR and western blot were used to detect the mRNA and protein expression of AQP9, ERK1/2, B-cell lymphoma-2 (Bcl-2), Bcl-associated x (Bax) in the myocardial tissue of rats. TTC and TUNEL staining were used to observe myocardial infarct size and apoptosis of myocardial cells in each group. Compared with control group, the levels of heart rate, left ventricular end-diastolic pressure, TNF-α, and IL-6 were increased in each group of rats with MI (all $p < 0.05$), while the levels of systolic blood pressure, diastolic blood pressure, mean arterial pressure, left ventricular systolic pressure, and IL-10 were significantly decreased (all $p < 0.05$). The mRNA and protein expression levels of AQP9, ERK1/2 phosphorylation and Bax were significantly increased, as well as the myocardial infarct size, apoptosis index of myocardial tissue (all $p < 0.05$), the mRNA and protein expression levels of Bcl-2 were significantly decreased (all $p < 0.05$). The AQP9 gene knock-down or exogenous administration of the ERK1/2 inhibitor U0126 could improve the above indexes. However, the combination of AQP9 gene knock-down and U0126 showed no further effect. Silencing AQP9 gene can inhibit the activation of ERK1/2 signaling pathway, attenuate the inflammatory response in rats with MI, inhibit apoptosis of myocardial cells, and improve cardiac function.

Keywords AQP9 · ERK1/2 · Myocardial infarction · Inflammatory response

Introduction

Myocardial infarction (MI), refers to myocardial necrosis caused by long-term hypoxia and ischemia [1, 2]. Clinically, MI patients are often accompanied by symptoms such as fever, pain, and increased white blood cell count [3]. In severe cases, MI patients can be complicated by heart failure, shock, and even threaten patient's life [4]. At present, the disease is mainly treated by early reperfusion to reduce infarct size, promote the reduction of left ventricular load, and avoid myocardial remodeling [5, 6]. In recent years, more and more studies have found that the inflammatory response mediated by immune cells plays an important role

Xingmei Huang, Xiaobin Yu are co-first authors and have contributed equally to this work.

✉ Xiangjun Yang
yangxiangjun62@163.com

[1] Department of Cardiology, The First Affiliated Hospital of Soochow University, No. 188 Shizi Road, Suzhou 215006, Jiangsu, China

[2] Department of Vascular Surgery, The Second Affiliated Hospital of Soochow University, Suzhou, Jiangsu, China

in the pathogenesis of MI [7]. Therefore, it is of great significance to investigate the changes of inflammatory response after MI for the treatment of this disease.

Aquaporins (AQPs) refer to the small molecular protein family distributed in cell membrane, which can promote the permeability of cell membrane, and it is of great significance in maintaining the water balance of cells [8]. AQP2, AQP6, AQP7, and AQP9 are all important members of their family [9]. Numerous studies on heart failure have confirmed that the expression of AQP2 is significantly increased in the rats model of heart failure, and AQP2 is a promotive factor in the pathogenesis of chronic and congestive heart failure [10]. AQP9 is located on the chromosome 15 (q22.1–22.2) and consists of 5 introns and 6 exons. The distribution of AQP9 in cells is mainly located in the vascular endothelial cells, which can transport not only water and glycerol, but also pyrimidines and lactic acid. AQP9 has been extensively studied in the field of neurological and cancer, Chen Q confirmed in the study that AQP9 could mediate the involvement of extracellular signal-regulated kinase1/2 (ERK1/2) signaling pathway in the progression of prostate cancer and silencing AQP9 could significantly inhibit the activation of ERK1/2 signaling pathway and reduce the proliferation and invasion of prostate cancer cells [11].

In recent years, study has also found that the expression level of AQP9 gene is significantly increased in patients with infective endocarditis and heart failure, and the expression level of AQP9 gene is closely related to the severity and prognosis of patients [12]. However, whether AQP9 is involved in the onset of MI has not been fully clarified. ERK1/2 signaling pathway plays an important regulatory role in the pathogenesis of MI, and inhibiting the activation of ERK1/2 signaling pathway is of great significance in reducing ventricular remodeling and improving cardiac function [13]. The aim of this study was to investigate the effect of AQP9 and ERK1/2 signaling pathway on inflammatory response and cardiac function in rats with MI.

Materials and methods

Experimental animals and grouping

A total of 65 healthy male Sprague–Dawley (SD) rats (purchased from Shanghai Slack Laboratory Animal Co., Ltd.), aged 8 weeks and weighing 180–200 g were selected in this research. Ten of the sixty-five rats were randomly selected as the control group (sham operation group, MI modeling sham operation). The remaining 55 rats were constructed rats model of MI and were divided into 5 groups: model group (MI modeling), NC group (MI modeling, tail vein injection of AQP9 negative control sequence vector), AQP9 shRNA group (MI modeling, tail vein injection of AQP9 shRNA plasmid vector), U0126 group (MI modeling, tail vein injection of ERK signaling pathway inhibitor), and AQP9 shRNA + U0126 group. The required plasmids were purchased from Shanghai Jiman Biotechnology Co., Ltd. All the rats were fed with normal diet and were allowed to drink water freely. The feeding room was guaranteed to get 12 h of light and dark every day. This experiment was approved by the Animal Ethics Committee of The First Affiliated Hospital of Soochow University and all animal experiments followed the Declaration of Helsinki.

Animal modeling and plasmid transfection

The rats model of MI was prepared according to references [14]. The rats were first weighed and then injected with 3% pentobarbital sodium at a dose of 30 mg/kg. After fixing the rats, a 1.2 cm incision was made on the left chest position. The fourth intercostal space was exposed after blunt dissection of the chest muscles. The small hemostatic forceps were used to make a small opening in the fourth intercostal space and the pleura and pericardium were torn. The left anterior descending coronary artery was ligated at 2 mm on the lower right horizontal line of the left atrial appendage with a 6–0 silk thread after the heart was exposed. Then heart was immediately placed in the chest cavity. The prepared plasmid (100 pmol per rat) was quickly injected into the tail vein of the rats with a 1 mL syringe. The cotton swab was used to clean the blood and effusion in the chest cavity. After confirming that there was no bleeding, the chest cavity was quickly merged, the upper and lower ribs were tightly aligned and sutured, and the muscles were aligned layer by layer and the skin was sutured.

Criteria for successful modeling: the anterior wall of the left ventricle turned pale, and the limb leads with 2 or more in the electrocardiogram were uplifted by 0.2 mV in ST segment. Rats in the control group were only for seton, and no coronary artery ligation was conducted. All rats were injected with penicillin for anti-infective treatment after suturing the skin.

Determination of hemodynamics and cardiac function

On the 7th day of MI modeling, 400 μL of blood samples was collected from the tail veins of rats in each group. The blood samples were stored at room temperature for 2 h and centrifuged at 3,000 r/min for 15 min at 4 °C, and the supernatant was collected and stored at – 80 °C for detection of AQP9 protein and inflammation factor [tumour necrosis factor-α (TNF-α), interleukin-6 (IL-6), interleukin-10 (IL-10)] level by ELISA. After blood collection, intraperitoneal injection of 3% phenobarbital sodium (60 mg/kg) was performed to anesthetize rats. After fixation, the right common carotid artery was isolated and inserted into a catheter filled with heparin

0.9% sodium chloride solution. Powerlab5 physiological recorder (ADInstruments Company, Australia) was connected and heart rate (HR), systolic blood pressure (SBP), diastolic blood pressure (DBP) and mean arterial pressure (MAP) were recorded. The catheter was further inserted into the left ventricle, and left ventricular end-diastolic pressure (LVEDP), left ventricular systolic pressure (LVSP) were measured. The rats were sacrificed by injecting 10% KCL into the femoral vein, and the heart was quickly removed, and part of myocardium in the myocardial infarct area was frozen and stored. The remaining myocardium was fixed in 10% formaldehyde solution for 24 h at 4 °C, embedded in paraffin, and stored at – 20 °C.

ELISA

The serum of each group was centrifuged at 3000 r/min for 30 min. AQP9, TNF-α, IL-6, and IL-10 levels were detected according to the instructions of AQP9 ELISA kit (ab15129, Abcam, UK), TNF-α ELISA kit (ab100747, Abcam, UK), IL-6 ELISA kit (ab100712, Abcam, UK), IL-10 ELISA kit (ab108870, Abcam, UK). After the detection, the OD values of each hole at 450 nm were read by ELISA (BioTek Synergy 2, USA). The abscissa coordinates were the concentration of the standard substance and the ordinate coordinates were the OD values. The standard curves were drawn.

Real-time quantitative PCR (qRT-PCR)

According to the instructions of Trizol (Invitrogen Company, USA), the total RNA of myocardial tissue in each group was extracted. RNA was dissolved by ultra-pure water containing diethylpyrocarbonate. The OD values at 260 nm and 280 nm were measured by means of an ND-1000 UV/Vis spectrophotometer (Nanodrop Company, USA), and the total RNA concentration was determined and stored at – 80 °C for use. The qRT-PCR primers were designed according to the PubMed database and Primer Premier 5.0, and then synthesized by Huada Gene Co., Ltd. See Table 1. The cDNA was synthesized using a reverse transcription kit, and the reverse transcriptase was inactivated by a warm bath at 80 °C for 5 min. The PCR system was 25 μL in all, and the internal reference was GAPDH. Reaction conditions: pre-denaturation at 95 °C for 10 min, 94 °C for 30 s, 59 °C for 30 s, 72 °C for 30 s, with 40 cycles in total. The reliability of the PCR results was evaluated by the dissolution curve, and the CT value (inflection point of the amplification dynamic curve), $\Delta Ct = CT$ (target gene) – CT (internal reference), $\Delta\Delta Ct = \Delta Ct$ (experimental group) - ΔCt (control group) were calculated by the relative quantitative method, and the relative expression amount of each target gene was expressed by $2^{-\Delta\Delta Ct}$. The experiment was repeated 3 times and averaged.

Table 1 qRT-PCR primer sequences

Target gene	Primer sequences′
AQP9	F: 5′-AAATAAACCTCCTTGGCCTGA-3′
	R: 5′-GCAACAAACATCACCACACC-3′
ERK1	F: 5′-CTGGCTTTCTGACCGAGTATGTG -3′
	R: 5′-CAATTTAGGTCCTCTTGGGATG-3′
ERK2	F: 5′-GACATGGAGCTGGACGACTTAC-3′
	R: 5′-GGGACACCGACATCTGAACG-3′
Bax	F: 5′-AGCTGCAGAGGATGATTGCT-3′
	R: 5′-CTGATCAGCTCGGGCACTTTA-3′
Bcl-2	F: 5′-GCCTCCTCACCTTTCAGCAT-3′
	R: 5′-CACTCGTAGCCCTCTGTGAC-3′
GAPDH	F: 5′-GCGCCCTTGGCTAAGGTTAT-3′
	R: 5′-AGGCCATACCAGTCAGCTTG-3′

AQP9 aquaporin 9, *ERK1* extracellular signal-regulated kinase1, *ERK2* extracellular signal-regulated kinase2, *Bcl-2* B-cell lymphoma-2, *Bax* Bcl- associated x

Western blot

After extracting myocardial tissue from each group, pre-cooled tissue lysis buffer RIPA (containing 1% protease inhibitor) was added and lysed on ice. After centrifugation at 12,000 r/min for 30 min at 4 °C, the supernatant was collected and the protein concentration was determined by means of a BCA kit (20201ES76, YEASEN, China). A total of 50 μg of protein was extracted, and the protein was separated by 10% SDS polyacrylamide gel electrophoresis (SDS-PAGE), and the separated protein was transferred to a nitrocellulose membrane (ZY-160FP, Zeye Bio, China). After taking out the membrane, 5% skim milk powder was added and sealed at room temperature for 2 h, and rinsed with TBS buffer for 3 times, 10 min each time. The diluted primary antibody rabbit anti-rat AQP9 (1:1,000, ab191056, abcam, UK), p-ERK1/2 (1:1,000, ab201015, Abcam, UK), Bcl- associated x (Bax) (1:1,000, ab32503, Abcam, UK), B-cell lymphoma-2 (Bcl-2) (1:1,000, ab692, Abcam, UK), GAPDH (1:1,000, ab181602, Abcam, UK) were incubated overnight at 4 °C. The membrane was rinsed with TBST for 3 times at 37 °C, 10 min each time. Secondary anti-HRP-labeled IgG goat anti-rabbit polyclonal antibody (1:500, ab20272, Abcam, UK) was added and shaken at 37 °C for 1 h, and rinsed the membrane with TBS for 3 times, 10 min each time. The membrane was reacted with ECL solution (ECL808-25, Biomiga, USA) for 1 min at room temperature. After the liquid was removed, the results were observed by X-ray machine (36209ES01, Qianchen Bio, China). GAPDH was used as internal reference, and the ratio of gray value of target band and internal reference band was used as the relative expression amount of protein.

Detection of myocardial infarct size in tissues by TTC staining

The myocardial tissue of each group was taken out and cut into 2 mm sections, and placed in TTC dye solution (Shanghai Hanheng Biological Research Institute, China). Then it was shaken in the dark, stained for 5–10 min at 37 °C and rinsed twice with tap water for 1 min each time. Next fixed it with 10% formaldehyde for 10 min. The result was that the infarct area showed white and non-infarct area showed red. The infarct size was measured by Image Pro Plus 6.0 software, and the percentage of infarct area in the total section was calculated.

Detection of apoptosis in tissues by TUNEL staining

The myocardial tissue sections of each group were dehydrated with 100%, 95%, 90%, 80%, and 70% gradient alcohol after xylene dewaxing, and then soaked with 3% hydrogen peroxide methanol to remove endogenous peroxidase. After the slices were fixed, they were placed in 0.1% Triton X-100 solution (Sigma Company, USA) transparentizing for 3 min and rinsed with PBS. According to the instructions of TUNEL detection kit (Roche, Basel, Switzerland), 50 μL of Tunel reaction solution (the ratio of enzyme solution and label solution was 1:9) was added reacting for 50 min, rinsed with PBS for 5 min, 3 times. After drying, 50 μL of transforming agent-POD was added, and it was incubated at 37 °C for 30 min, developing with DAB for 3 min, and rinsed with PBS for 5 min, 3 times. Then drying it again, hematoxylin counterstained for 3 s, sealed with neutral gum, and the staining results were observed under high-power microscope. Randomly selected 5 fields of view, the apoptotic rate (100%) in each field of view = (apoptotic cells/total cells) × 100%.

Statistical analysis

SPSS 18.0 software was used to analyze the experimental data. The measurement data were expressed as mean ± standard deviation. One-way analysis of variance (ANOVA) was used for comparison among groups, and *t* test was used for comparison between groups. There is a significant difference at $p < 0.05$.

Results

Results of animal modeling

Five rats died of excessive blood loss, arrhythmia and lung injury during the process of modeling, and 50 rats were successfully modeled, with a successful modeling rate of 90.91%. The 50 successfully modeled rats were divided into 5 groups: model group (MI modeling), NC group (MI modeling, tail vein injection of AQP9 negative control sequence vector), AQP9 shRNA group (MI modeling, tail vein injection of AQP9 shRNA plasmid vector), U0126 group (MI modeling, tail vein injection of ERK1/2 signaling pathway inhibitor), and AQP9 shRNA + U0126group, 10 in each group. The control group was MI modeling sham operation group.

The results of ELISA showed that compared with control group, the AQP9 levels of the model group, NC group, AQP9 shRNA group, U0126 group and AQP9 shRNA + U0126 group in peripheral blood were significantly increased (all $p < 0.05$). Compared with model group, the AQP9 levels of AQP9 shRNA group and AQP9 shRNA + U0126 group in peripheral blood were significant decreased (all $p < 0.05$). Compared with model group, there were no significant differences between NC group and U0126 group (all $p > 0.05$). Compared with AQP9 shRNA group, there were no significant differences in the AQP9 levels between AQP9 shRNA + U0126 group and U0126 group (all $p > 0.05$). See Fig. 1.

The results of qRT-PCR showed that compared with control group, the mRNA expression levels of AQP9 and ERK1/2 in the myocardial tissue of the model group, NC group, AQP9 shRNA group, U0126 group, and AQP9 shRNA + U0126 group were significantly increased (all $p < 0.05$). Compared with model group, the mRNA expression levels of AQP9 and ERK1/2 in the myocardial tissue of the AQP9 shRNA group and AQP9 shRNA + U0126 group were significantly decreased (all $p < 0.05$). There was no significant difference in the mRNA expression levels of AQP9 between model group and U0126 group ($p > 0.05$), while the mRNA expression level of ERK1/2 in U0126 group was

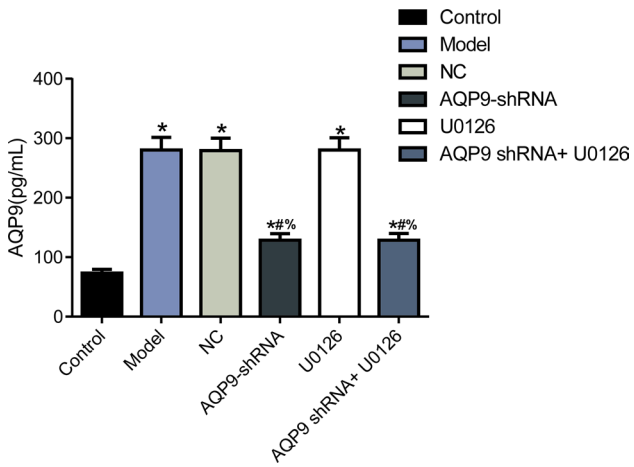

Fig. 1 ELISA detection of AQP9 level in peripheral blood of rats in each group. Compared with control group, $^{*}p < 0.05$. Compared with model group, $^{\#}p < 0.05$. Compared with NC group, $^{\%}p < 0.05$. AQP9: aquaporin 9

significantly decreased than in model group ($p < 0.05$). There was no significant difference in the mRNA expression levels of AQP9 and ERK1/2 between model group and NC group (both $p > 0.05$). There was no significant difference in the mRNA expression levels of AQP9 and ERK1/2 between AQP9 shRNA group and AQP9 shRNA + U0126 group (both $p > 0.05$). See Fig. 2.

The results of western blot showed that compared with control group, the protein expression levels of AQP9 and ERK1/2 phosphorylation in the myocardial tissue of the model group, NC group, AQP9 shRNA group, U0126 group and AQP9 shRNA + U0126 group were significantly increased (all $p < 0.05$). Compared with model group, the protein expression levels of AQP9 and ERK1/2 phosphorylation in the myocardial tissue of the AQP9 shRNA group and AQP9 shRNA + U0126 group were significantly decreased (all $p < 0.05$). There was no significant difference in the protein expression level of AQP9 between model group and U0126 group ($p > 0.05$), while the protein expression level of ERK1/2 in U0126 group was significantly decreased than in model group ($p < 0.05$). There was no significant difference in the protein expression levels of AQP9 and ERK1/2 phosphorylation between model group and NC group (both $p > 0.05$). There was no significant difference in the protein expression levels of AQP9 and ERK1/2 phosphorylation between AQP9 shRNA group and AQP9 shRNA + U0126 group (both $p > 0.05$). See Fig. 3.

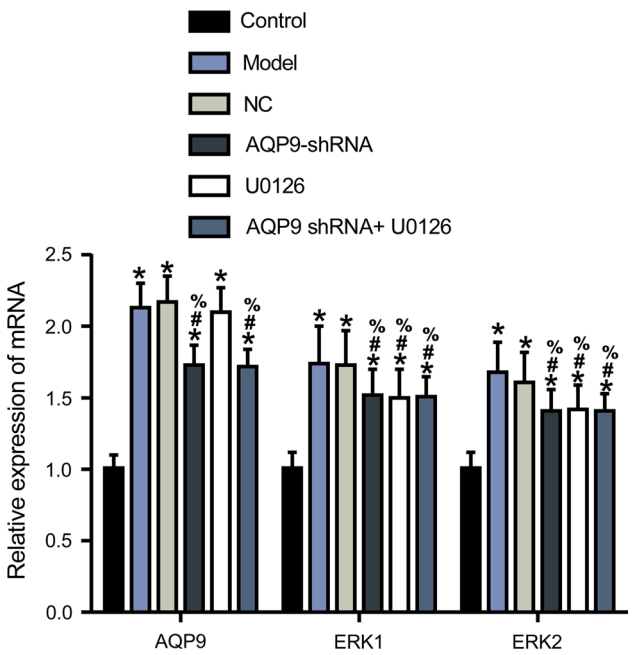

Fig. 2 qRT-PCR detection of the mRNA expression of AQP9 and ERK1/2 in the myocardial tissue of rats in each group. Compared with control group, $^{*}p < 0.05$. Compared with model group, $^{\#}p < 0.05$. Compared with NC group, $^{\%}p < 0.05$. *qRT-PCR* real-time quantitative PCR, *AQP9* aquaporin 9, *ERK1/2*: extracellular signal-regulated kinase 1/2

Determination of hemodynamics and cardiac function in myocardial tissue of rats in each group

Comparison of hemodynamics and cardiac function in myocardial tissue of each group of rats was shown in Table 2. Compared with control group, the HR of rats in model group, NC group, AQP9 shRNA group, U0126 group, and AQP9 shRNA + U0126 group was significantly accelerated, the LVEDP was significantly increased, and the SBP, DBP, MAP, and LVSP were significantly decreased (all $p < 0.05$). Compared with model group, the HR of rats in AQP9 shRNA group, U0126 group and AQP9 shRNA + U0126 group was significantly slower, the LVEDP was significantly decreased, and the SBP, DBP, MAP, and LVSP were significantly increased (all $p < 0.05$). Compared with NC group, the HR of rats in AQP9 shRNA group, U0126 group and AQP9 shRNA + U0126 group was significantly slower, the LVEDP was significantly decreased, and the SBP, DBP, MAP, and LVSP were significantly increased (all $p < 0.05$). There was no significant difference between model group and NC group ($p > 0.05$). Compared with AQP9 shRNA group, there were no significant differences between AQP9 shRNA + U0126 group and U0126 group (all $p > 0.05$).

Effect of silencing AQP9 gene inhibits the activation of ERK1/2 signaling pathway on inflammatory response of rats with MI

The results of ELISA showed that compared with control group, the levels of TNF-α and IL-6 in the model group, NC group, AQP9 shRNA group, U0126 group and AQP9 shRNA + U0126 group were significantly increased (all $p < 0.05$), while IL-10 levels were significantly decreased (all $p < 0.05$). Compared with model group, the levels of TNF-α and IL-6 in the AQP9 shRNA group, U0126 group, and AQP9 shRNA + U0126 group were significantly decreased (all $p < 0.05$), while IL-10 levels were significantly increased ($p < 0.05$). Compared with NC group, the levels of TNF-α and IL-6 in the AQP9 shRNA group, U0126 group and AQP9 shRNA + U0126 group were significantly decreased (all $p < 0.05$), while IL-10 levels were significantly increased ($p < 0.05$). There was no significant difference in the levels of inflammatory factors between model group and NC group (both $p > 0.05$). Compared with AQP9 shRNA group, there were no significant differences in the levels of inflammatory factors between AQP9 shRNA + U0126 group and U0126 group (all $p > 0.05$). See Fig. 4.

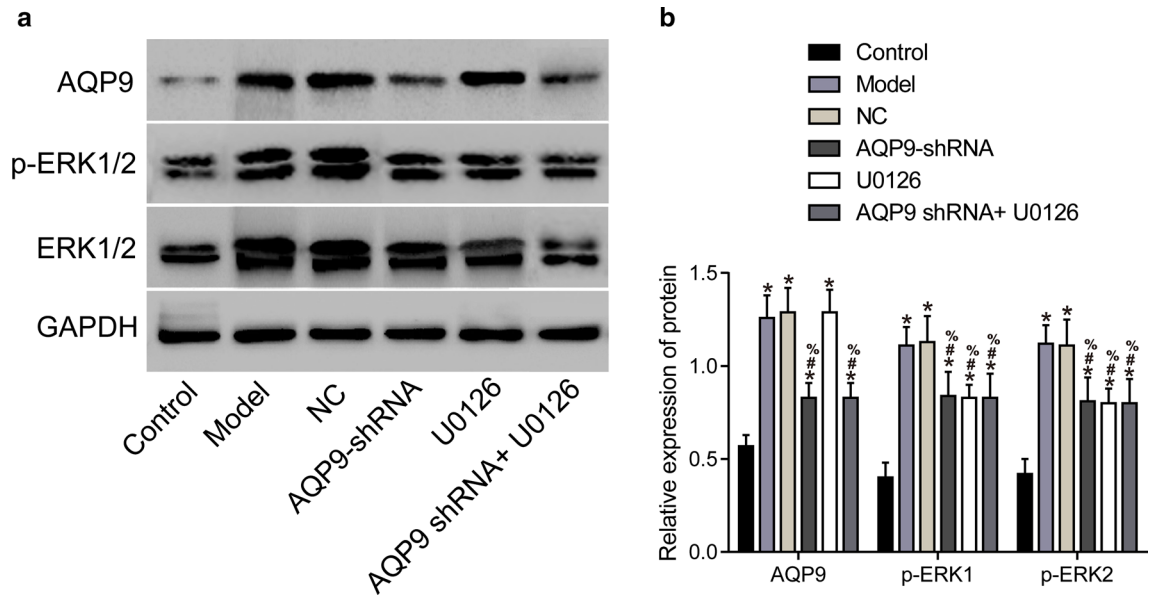

Fig. 3 Western blot detection of the protein expression of AQP9 and ERK1/2 phosphorylation in the myocardial tissue of rats in each group. **a** Western blot was used to detect the protein electrophoresis bands in the myocardial tissues of rat in each group. **b** Western blot was used to detect the protein expression level in the myocardial tissues of rats in each group. Compared with control group, $^{*}p<0.05$. Compared with model group, $^{\#}p<0.05$. Compared with NC group, $^{\%}p<0.05$. *AQP9* aquaporin 9, *ERK1/2* extracellular signal-regulated kinase1/2

Table 2 Comparison of hemodynamics and cardiac function in myocardial tissue of mice in each group

	Control group	Model group	NC group	AQP9-shRNA group	U0126 group	AQP9 shRNA + U0126 group
HR (time/min)	347.34 ± 30.02	436.54 ± 40.85*	432.14 ± 39.14*	382.25 ± 37.21$^{*\#\%}$	380.16 ± 36.24$^{*\#\%}$	381.16 ± 34.26$^{*\#\%}$
SBP (mmHg)	137.51 ± 12.42	108.96 ± 10.82*	107.46 ± 10.32*	119.34 ± 11.15$^{*\#\%}$	120.15 ± 11.56$^{*\#\%}$	120.15 ± 11.14$^{*\#\%}$
DBP (mmHg)	109.83 ± 11.35	81.55 ± 8.92*	82.05 ± 8.52*	93.52 ± 9.10$^{*\#\%}$	94.32 ± 9.52$^{*\#\%}$	93.52 ± 9.51$^{*\#\%}$
MAP (mmHg)	114.57 ± 10.98	90.37 ± 7.24*	91.53 ± 7.33*	101.92 ± 8.44$^{*\#\%}$	102.62 ± 8.03$^{*\#\%}$	101.84 ± 8.16$^{*\#\%}$
LVSP (mmHg)	152.89 ± 15.54	108.64 ± 10.25*	107.01 ± 10.16*	135.21 ± 12.59$^{*\#\%}$	133.01 ± 11.05$^{*\#\%}$	132.21 ± 12.41$^{*\#\%}$
LVEDP (mmHg)	6.21 ± 1.01	22.23 ± 2.33*	22.31 ± 2.42*	14.13 ± 1.42$^{*\#\%}$	14.53 ± 1.36$^{*\#\%}$	14.13 ± 1.32$^{*\#\%}$

HR heart rate, *SBP* systolic blood pressure, *DBP* diastolic blood pressure, *MAP* mean arterial pressure, *LVSP* left ventricular systolic pressure, *LVEDP* left ventricular end-diastolic pressure

Compared with control group, $^{*}p<0.05$. Compared with model group, $^{\#}p<0.05$. Compared with NC group, $^{\%}p<0.05$

Effect of silencing AQP9 gene inhibits the activation of ERK1/2 signaling pathway on apoptosis of myocardial cells of rats with MI

The results of qRT-PCR showed that compared with control group, the mRNA expression levels of Bax in the myocardial tissue of the model group, NC group, AQP9 shRNA group, U0126 group and AQP9 shRNA + U0126 group were significantly increased (all $p<0.05$), and the mRNA expression levels of Bcl-2 were significantly decreased (all $p<0.05$). Compared with model group, the mRNA expression levels of Bax in the myocardial tissue of the AQP9 shRNA group, U0126 group and AQP9 shRNA + U0126 group were significantly decreased (all $p<0.05$), and the mRNA expression levels of Bcl-2 were significantly increased (all $p<0.05$). Compared with NC group, the mRNA expression levels of Bax in the myocardial tissue of the AQP9 shRNA group, U0126 group, and AQP9 shRNA + U0126 group were significantly decreased (all $p<0.05$), and the mRNA expression levels of Bcl-2 were significantly increased (all $p<0.05$). There was no significant difference between model group and NC group (both $p>0.05$). Compared with AQP9 shRNA group, there were no significant differences between AQP9 shRNA + U0126 group and U0126 group (all $p>0.05$). See Fig. 5.

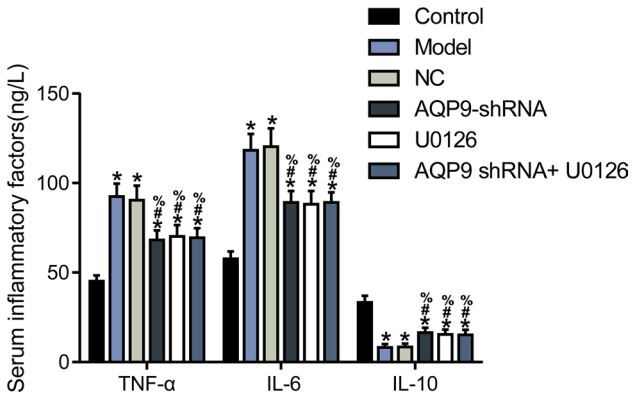

Fig. 4 ELISA detection of inflammatory factors (TNF-α, IL-6, and IL-10) levels in peripheral blood of rats in each group. Compared with control group, $^{*}p<0.05$. Compared with model group, $^{\#}p<0.05$. Compared with NC group, $^{\%}p<0.05$. *TNF-α* tumour necrosis factor-α, *IL-6* interleukin-6, and *IL-10* interleukin-10

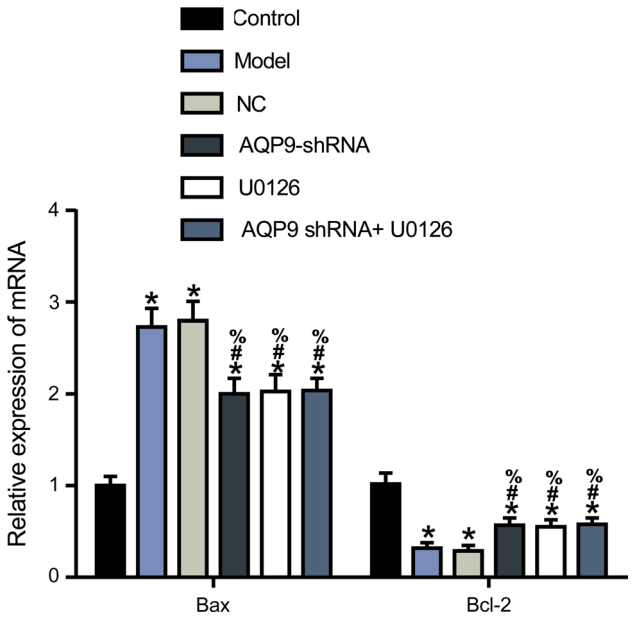

Fig. 5 qRT-PCR detection of the mRNA expression of apoptosis gene Bax and Bcl-2 in the myocardial tissue of rats in each group. Compared with control group, $^{*}p<0.05$. Compared with model group, $^{\#}p<0.05$. Compared with NC group, $^{\%}p<0.05$. qRT-PCR: Real-time quantitative PCR. Bax: Bcl-associated x. Bcl-2: B-cell lymphoma-2

The results of western blot showed that compared with control group, the protein expression levels of Bax in the myocardial tissue of the model group, NC group, AQP9 shRNA group, U0126 group and AQP9 shRNA + U0126 group were significantly increased (all $p<0.05$), and the protein expression levels of Bcl-2 were significantly decreased (all $p<0.05$). Compared with model group, the protein expression levels of Bax in the myocardial tissue of the AQP9 shRNA group, U0126 group and AQP9 shRNA + U0126 group were significantly decreased (all $p<0.05$), and the protein expression levels of Bcl-2 were significantly increased (all $p<0.05$). Compared with NC group, the protein expression levels of Bax in the myocardial tissue of the AQP9 shRNA group, U0126 group and AQP9 shRNA + U0126 group were significantly decreased (all $p<0.05$), and the protein expression levels of Bcl-2 were significantly increased (all $p<0.05$). There was no significant difference in protein expression level between model group and NC group (both $p>0.05$). Compared with AQP9 shRNA group, there were no significant differences in protein expression level between AQP9 shRNA + U0126 group and U0126 group (all $p>0.05$). See Fig. 6.

The results of TUNEL staining showed that compared with control group, the apoptotic index of myocardial tissue in the model group, NC group, AQP9 shRNA group, U0126 group and AQP9 shRNA + U0126 group was significantly increased (all $p<0.05$). Compared with model group, the apoptotic index of myocardial tissue in the AQP9 shRNA group, U0126 group and AQP9 shRNA + U0126 group was significantly decreased (all $p<0.05$). Compared with NC group, the apoptotic index of myocardial tissue in the AQP9 shRNA group, U0126 group and AQP9 shRNA + U0126 group was significantly decreased (all $p<0.05$). There was no significant difference between model group and NC group in the apoptotic index of myocardial tissue ($p>0.05$). Compared with AQP9 shRNA group, there were no significant differences in the apoptotic index of myocardial tissue between AQP9 shRNA + U0126 group and U0126 group (all $p>0.05$). See Fig. 7.

Effect of silencing AQP9 gene inhibits the activation of ERK1/2 signaling pathway on myocardial infarct size of rats with MI

Myocardial infarct size was detected by TTC, and comparison of myocardial infarct size in each group was shown in Fig. 8. Compared with control group, the myocardial infarct size of the model group, NC group, AQP9 shRNA group, U0126 group, and AQP9 shRNA + U0126 group was significantly increased (all $p<0.05$). Compared with model group, the myocardial infarct size of the AQP9 shRNA group, U0126 group and AQP9 shRNA + U0126 group was significantly decreased (all $p<0.05$). Compared with NC group, the myocardial infarct size of the AQP9 shRNA group, U0126 group and AQP9 shRNA + U0126 group were significantly decreased (all $p<0.05$). There was no significant difference in myocardial infarct size between model group and NC group ($p>0.05$). Compared with AQP9 shRNA group, there were no significant

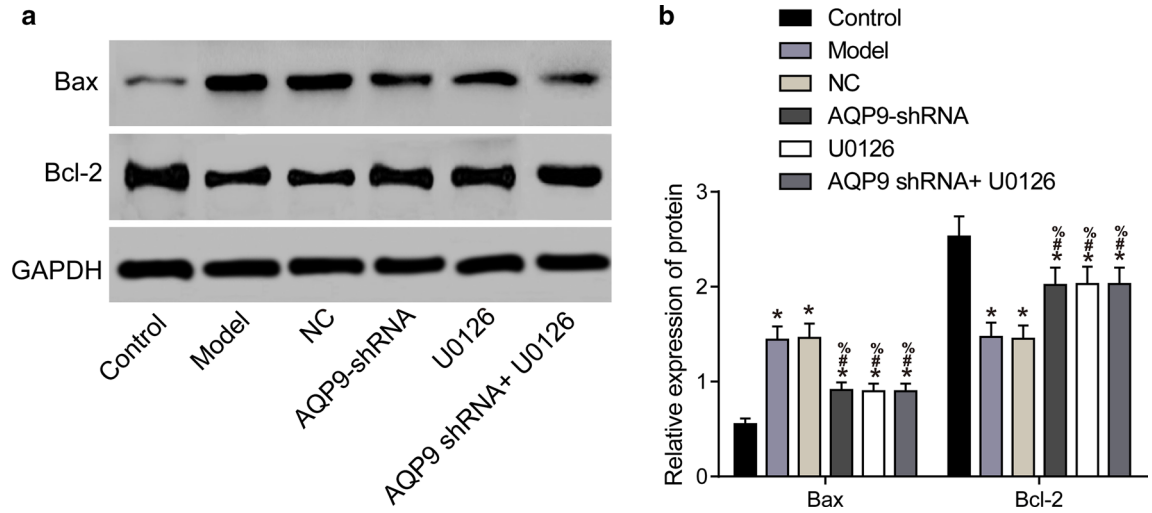

Fig. 6 Western blot detection of the protein expression of apoptosis gene Bax and Bcl-2 in the myocardial tissue of rats in each group. **a** Western blot was used to detect the protein electrophoresis bands in the myocardial tissues of rats in each group. **b** Western blot was used to detect the protein expression level in the myocardial tissues of rats in each group. Compared with control group, $^{*}p<0.05$. Compared with model group, $^{\#}p<0.05$. Compared with NC group, $^{\%}p<0.05$. *Bax* Bcl-associated x, *Bcl-2* B-cell lymphoma-2

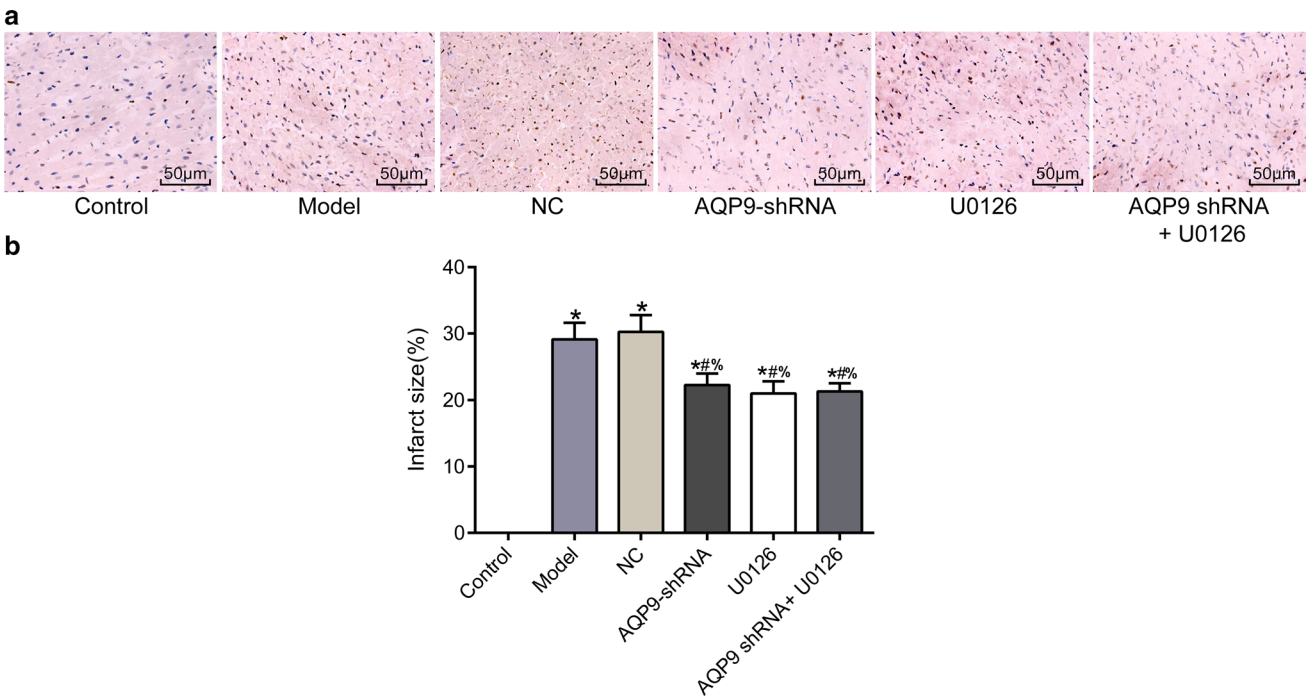

Fig. 7 Apoptosis of myocardial tissue in rats (× 200). **a** TUNEL staining results of the myocardial tissue of rats in each group. **b** TUNEL staining was used for the detection of apoptotic index in the myocardial tissue of rats in each group. Compared with control group, $^{*}p<0.05$. Compared with model group, $^{\#}p<0.05$. Compared with NC group, $^{\%}p<0.05$

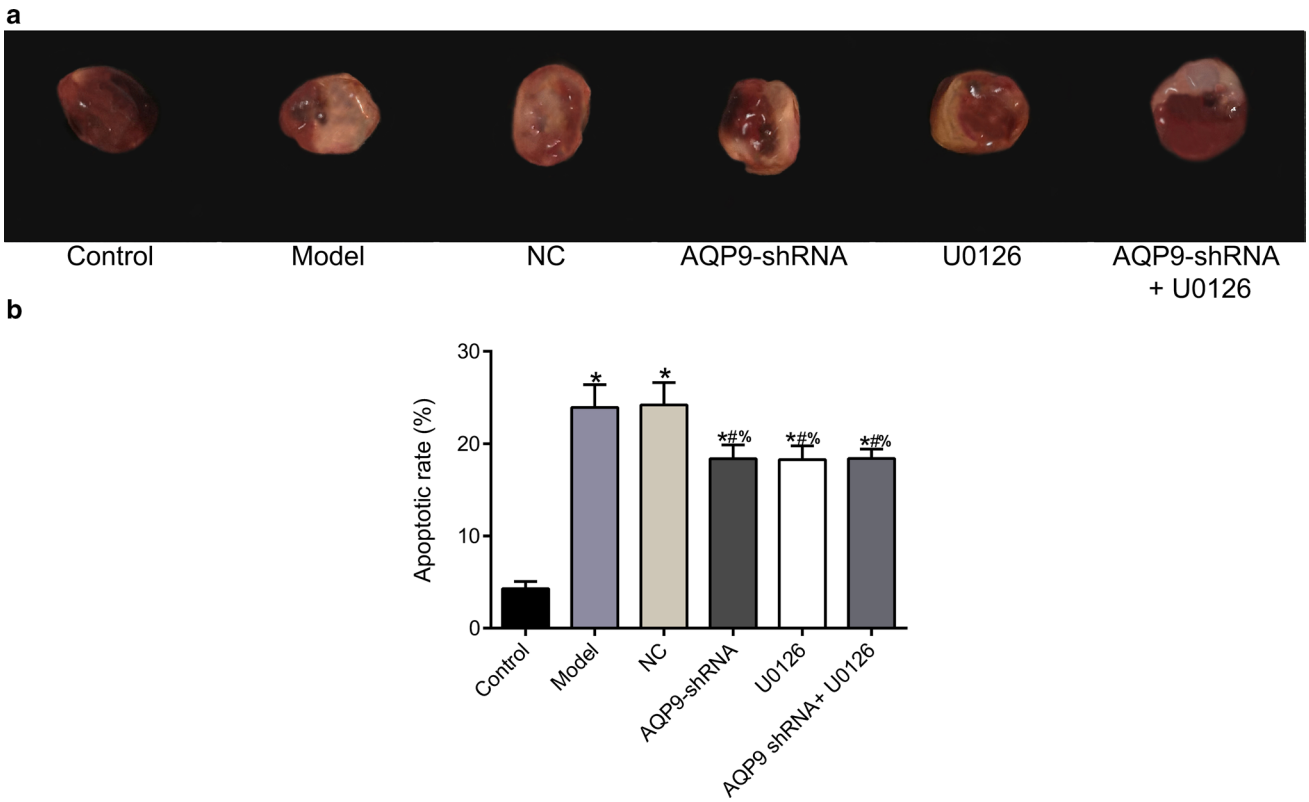

Fig. 8 Comparison of myocardial infarction in rats of each group. **a** Results of myocardial tissue stained by TTC in rats of each group. **b** Percentage of myocardial infarct size in rats of each group. Compared with control group, $^{*}p < 0.05$. Compared with model group, $^{\#}p < 0.05$. Compared with NC group, $^{\%}p < 0.05$

differences in myocardial infarct size between AQP9 shRNA + U0126 group and U0126 group ($p > 0.05$).

Discussion

Myocardial infarction (MI) is the main cause of heart failure in clinic at present. With the deepening of research on cardiac pathophysiology in recent years, more and more attention has been paid to the role of inflammatory mediators and anti-inflammatory therapy in MI [15, 16]. Tan J found in the animal study that excessive secretion of inflammatory factors could aggravate the damage of myocardial ischemia, inhibit the inflammatory response in MI, significantly improve myocardial remodeling, and improve cardiac function in rats with MI [17]. From the point of molecular biology, this study constructed the rats model of MI and investigated the correlation between AQP9-mediated ERK1/2 signaling pathway and MI. The results confirmed that AQP9 gene silencing could inhibit the activation of ERK1/2 signaling pathway and improve inflammatory response and cardiac function in rats.

After MI, the contractility and pumping function of the myocardium often decline, which will further lead to the decrease of LVSP and arterial pressure (SBP, DBP, and MAP), and the increase of HR and LVEDP [18, 19]. In this study, after treatment of rats in each group, it was found that the ventricular contractility of AQP9 shRNA group was significantly enhanced, and each index of cardiac function was also significantly improved. Proper inflammatory response plays an important role in the repair of myocardial cell injury, but excessive inflammatory response may aggravate ventricular remodeling and even cause heart failure [20, 21]. Neutrophils have been confirmed to be an important cellular basis in the process of inflammatory response after MI [22]. The continuous activation of chemokines and activation of complement system in infarct area can induce a large mount secretion of neutrophils. The activation of neutrophils can continuously increase the content of pro-inflammatory factors such as TNF-α and IL-6; the increase of pro-inflammatory mediators can further promote the prolongation of neutrophil survival, thereby further aggravating the inflammatory response [23]. In addition, excessive secretion of neutrophils can further inhibit the activation of anti-inflammatory mechanism of macrophages, and the secretion of anti-inflammatory factor IL-10 is decreasing [24]. ERK1/2 signaling pathway is an important pathway that

plays a regulatory role in various pathophysiological processes of the human body; generally, ERK1/2 is located in human cellular cytoplasm and transferred to the nucleus after being activated and regulates the activity of transcription factors, and ERK1/2 signaling pathway can be involved in various cell activities such as the regulation of proliferation and cell cycle [25]. In recent years, more and more studies have confirmed that the ERK1/2 signaling pathway can regulate the inflammatory response. Lv et al. confirmed in the study on the ERK1/2 signaling pathway and acute lung injury rats' lung function that inhibiting the activation of ERK1/2 signaling pathway could reduce the proliferation of airway smooth muscle induced by inflammatory response [26]. In a study of MI, Guo found that inhibition of ERK1/2 signaling pathway could significantly inhibit myocardial inflammatory response in rats with MI, thereby improving the process of myocardial remodeling and apoptosis of myocardial cells after MI [27]. In this study, compared with model group, the levels of TNF-α and IL-6 in AQP9 shRNA group and U0126 group were significantly decreased, while IL-10 levels were significantly increased. It is suggested that inhibition of AQP9 gene or activation of ERK1/2 signaling pathway can improve the inflammatory response of rats with MI and inhibit the secretion of pro-inflammatory factors, and has a significant protective effect on myocardial inflammatory response and cardiac function in rats with MI.

Massive apoptosis of myocardial cells is an important pathological basis for acute MI [28]. Liu found in the study that more than 80% of cell loss in the myocardial infarct area originated from the apoptosis of myocardial cells, which was the most important factor in the pathogenesis of MI [29]. The anti-apoptotic protein Bcl-2 and the pro-apoptotic protein Bax are the most important factors in the regulation of apoptosis, and the balance of their expression levels and functions is important for the survival of cells [30]. If there is a large increase in Bax but a significant decrease in Bcl-2 in myocardial cells, the apoptosis of myocardial cells is significantly increased [31]. In this study, silencing expression of AQP9 and inhibiting ERK1/2 signaling pathway can significantly enhance the expression of Bcl-2 and inhibit the expression of Bax. The significant decrease of ERK1/2 expression in the AQP9 shRNA group suggests that the inhibition of apoptosis by AQP9 gene silencing is mainly achieved by inhibiting ERK1/2 signaling pathway. TUNEL staining further confirmed the protective effect of AQP9 gene silencing on apoptosis of myocardial cells in rats with MI. TTC method was used to detect the myocardial infarct size of each group. It was found that compared with model group, the myocardial infarct size in the AQP9 shRNA group and U0126 group was significantly decreased, suggesting that AQP9 gene silencing plays an active protective role in MI.

In conclusion, AQP9 gene silencing can inhibit the activation of ERK1/2 signaling pathway, improve myocardial inflammatory response and cardiac function in rats with MI, and has an important protective effect on MI. AQP9 is expected to be an important target in the treatment of MI.

Acknowledgements This work was supported by National Natural Science Foundation of China (81700298).

Compliance with ethical standards

Conflict of interest The authors declare that they have no conflict of interest.

Ethical approval This experiment was approved by the Animal Ethics Committee of The First Affiliated Hospital of Soochow University. All animal experiments followed the Declaration of Helsinki. All applicable international, national, and/or institutional guidelines for the care and use of animals were followed.

References

1. Bainey KR, Fresco C, Zheng Y, Halvorsen S, Carvalho A, Ostojic M, Goldstein P, Gershlick AH, Westerhout CM, Van de Werf F, Armstrong PW, Investigators STREAM (2016) Implications of ischaemic area at risk and mode of reperfusion in ST-elevation myocardial infarction. Heart 102:527–533
2. Goto Y, Ishida M, Yamada A, Uno M, Nakamori S, Nagata M, Ichikawa Y, Kitagawa K, Ito M, Sakuma H (2016) Native T1 mapping allows for the accurate detection of the segments with chronic myocardial infarction in patients with known or suspected coronary artery disease. J Cardiovasc Magn Reson 18:70
3. Orlic D, Ostojic MC, Labudovic M (2015) TCT-245 The randomized physiologic assessment of thrombus aspiration in patients with acute myocardial Infarction with ST-segment slevation (PATA STEMI) trial: final results. J Am Coll Cardiol 66:B42–B43
4. Ouweneel DM, Eriksen E, Sjauw KD, van Dongen IM, Hirsch A, Packer EJ, Vis MM, Wykrzykowska JJ, Koch KT, Baan J, de Winter RJ, Piek JJ, Lagrand WK, de Mol BA, Tijssen JG, Henriques JP (2017) Percutaneous mechanical circulatory support versus intra-aortic balloon pump in cardiogenic shock after acute myocardial infarction. J Am Coll Cardiol 69:278–287
5. Pascual-Gil S, Simón-Yarza T, Garbayo E, Prosper F, Blanco-Prieto MJ (2015) Tracking the in vivo release of bioactive NRG from PLGA and PEG-PLGA microparticles in infarcted hearts. J Control Release 220:388–396
6. Greenberg H, McMaster P, Dwyer EM Jr (1984) Left ventricular dysfunction after acute myiocardial infarction: results of a prospective multicenter study. J Am Coll Cardiol 4:867–874
7. Alam MA, Subhan N, Rahman MM, Uddin SJ, Reza HM, Sarker SD (2014) Effect of citrus flavonoids, naringin and naringenin, on metabolic syndrome and their mechanisms of action. Adv Nutr 5:404–417
8. Meli R, Pirozzi C, Pelagalli A (2018) New perspectives on the potential role of aquaporins (AQPs) in the physiology of inflammation. Front Physiol 9:101
9. Sang YL, Nam YK, Yi KK (2017) Characterization and expression profiles of aquaporins (AQPs) 1a and 3a in mud loach *Misgurnus mizolepis*, after experimental challenges. Fish Aquat Sci 20:23

10. Cui X, Zhang J, Li Y, Sun Y, Cao J, Zhao M, Zhao Y, Zhao X, He Y, Han A (2015) Effects of Qili Qiangxin capsule on AQP2, V2R, and AT1R in rats with chronic heart failure. Evid Based Complement Alternat Med 2015:639450
11. Chen Q, Zhu L, Zheng B, Wang J, Song X, Zheng W, Wang L, Yang D, Wang J (2016) Effect of AQP9 expression in androgen-independent prostate cancer cell PC3. Int J Mol Sci 17:E738
12. Thuny F, Textoris J, Amara AB, Filali AE, Capo C, Habib G, Raoult D, Mege JL (2012) The gene expression analysis of blood reveals S100A11 and AQP9 as potential biomarkers of infective endocarditis. PLoS One 7:e31490
13. Sun SJ, Wu XP, Song HL, Li GQ (2015) Baicalin ameliorates isoproterenol-induced acute myocardial infarction through iNOS, inflammation, oxidative stress and P38MAPK pathway in rat. Int J Clin Exp Med 8:22063–22072
14. Gao E, Lei YH, Shang X, Huang ZM, Zuo L, Boucher M, Fan Q, Chuprun JK, Ma XL, Koch WJ (2010) A novel and efficient model of coronary artery ligation and myocardial infarction in the mouse. Circ Res 107:1445–1453
15. Vukomanovic V, Tadic M, Suzic-Lazic J, Kocijancic V, Celic V (2017) The relationship between heart rate variability and left ventricular layer-specific deformation in uncomplicated diabetic patients. Int J Cardiovasc Imaging 33:481–490
16. Shah AM, Claggett B, Sweitzer NK, Shah SJ, Anand IS, Liu L, Pitt B, Pfeffer MA, Solomon SD (2015) Prognostic importance of impaired systolic function in heart failure with preserved ejection fraction and the impact of spironolactone. Circulation 132:402–414
17. Tan J, Hua Q (2012) Correlations between serum inflammation factors and left ventricular remodeling in acute ST segment elevation myocardial infarction. Yonsei Med J 53:501–507
18. Arini PD, Valverde ER (2016) Beat-to-beat electrocardiographic analysis of ventricular repolarization variability in patients after myocardial infarction. J Electrocardiol 49:206–213
19. Ren J, Li C, Liu Y, Liu H, Dong Z (2018) Protective effect of dexmedetomidine against myocardial ischemia-reperfusion injury in rabbits. Acta Cir Bras 33:22–30
20. Yeh CF, Wang CH, Tsai PR, Wu CK, Lin YH, Chen YS (2015) Use of extracorporeal membrane oxygenation to rescue patients with refractory ventricular arrhythmia in acute myocardial infarction. Medicine (Baltimore) 94:e1241
21. Wan N, Liu X, Zhang XJ, Zhao Y, Hu G, Wan F, Zhang R, Zhu X, Xia H, Li H (2015) Toll-interacting protein contributes to mortality following myocardial infarction through promoting inflammation and apoptosis. Br J Pharmacol 172:3383–3396
22. Carbone F, Nencioni A, Mach F, Vuilleumier N, Montecucco F (2013) Pathophysiological role of neutrophils in acute myocardial infarction. Thromb Haemost 110:501–514
23. Montecucco F, Bauer I, Braunersreuther V, Bruzzone S, Akhmedov A, Lüscher TF, Speer T, Poggi A, Mannino E, Pelli G, Galan K, Bertolotto M, Lenglet S, Garuti A, Montessuit C, Lerch R, Pellieux C, Vuilleumier N, Dallegri F, Mage J, Sebastian C, Mostoslavsky R, Gayet-Ageron A, Patrone F, Mach F, Nencioni A (2013) Inhibition of nicotinamide phosphoribosyltransferase reduces neutrophil-mediated injury in myocardial infarction. Antioxid Redox Signal 18:630–641
24. Riesenberg K, Levy R, Katz A, Galkop S, Schlaeffer F (1997) Neutrophil superoxide release and interleukin 8 in acute myocardial infarction: distinction between complicated and uncomplicated states. Eur J Clin Invest 27:398–404
25. Tu XK, Yang WZ, Chen JP, Chen Y, Chen Q, Chen PP, Shi SS (2015) Repetitive ischemic preconditioning attenuates inflammatory reaction and brain damage after focal cerebral ischemia in rats: involvement of PI3K/Akt and ERK1/2 signaling pathway. J Mol Neurosci 55:912–922
26. Lv H, Zhu C, Liao Y, Gao Y, Lu G, Zhong W, Zheng Y, Chen W, Ci X (2015) Tenuigenin ameliorates acute lung injury by inhibiting NF-κB and MAPK signalling pathways. Respir Physiol Neurobiol 216:43–51
27. Guo C, Ma L (2015) TCTAP A-027 Panax Notoginseng Saponins safely boost cardiac function and anti-apoptosis in a myocardial infarction model in the RAT via the MEK/ERK1/2 pathway. J Am Coll Cardiol 65:S12
28. Xiao J, She Q, Wang Y, Luo K, Yin Y, Hu R, Huang K (2009) Effect of allopurinol on cardiomyocyte apoptosis in rats after myocardial infarction. Eur J Heart Fail 11:20–27
29. Liu Y, Yang H, Liu LX, Yan W, Guo HJ, Li WJ, Tian C, Li HH, Wang HX (2016) NOD2 contributes to myocardial ischemia/reperfusion injury by regulating cardiomyocyte apoptosis and inflammation. Life Sci 149:10–17
30. Liu M, Wang XR, Wang C, Song DD, Liu XH, Shi DZ (2013) Panax quinquefolium saponin attenuates ventricular remodeling after acute myocardial infarction by inhibiting chop-mediated apoptosis. Shock 40:339–344
31. Zhang D, Zhu L, Li C, Mu J, Fu Y, Zhu Q, Zhou Z, Liu P, Han C (2015) Sialyltransferase7A, a Klf4-responsive gene, promotes cardiomyocyte apoptosis during myocardial infarction. Basic Res Cardiol 110:28